

# Hybrid Flatness-Based Control of Dual Star Induction Machine Drive System for More Electrical Aircraft

Research paper

Mokhtar Nesri<sup>1,\*</sup>, Kamal Nounou<sup>2</sup>, Guedida Sifelislam<sup>2</sup>, Mohamed Fouad Benkhoris<sup>3</sup>, HOUARI Azeddine<sup>3</sup>

<sup>1</sup>Ecole superieur Ali Chabati, Reghaia Algiers, Algeria

<sup>2</sup>Ecole Militaire Polytechnique, LSEE UER-ELT, Bordj El-Bahri Algiers, Algeria

<sup>3</sup>IREENA Laboratory Université de Nantes, Nantes, France

Received: 14 October, 2023; Accepted: 30 November, 2023

**Abstract:** This paper develops a precise method control system for tracking control of a power drive system based on a multi-phase machine under motor parameter and load torque variations. By adding a simple feedforward term based on the flatness theory, a conventional flux oriented control (FOC) can be enforced to have a perfect tracking performance under model parameter and load torque variations. Hence, a hybrid flatness-based control (HFBC) technique is applied to the control of a dual star induction machine (DSIM) and compared to a classical vector control strategy regarding tracking behaviour, robustness, and perturbations rejection. Finally, the simulation and experimental results are provided to verify the effectiveness of the proposed HFBC under uncertainties such as motor parameter and load torque variations. Furthermore, an enhancement of the drive system's control performances is demonstrated by the improvement of the technique of separation of the objectives of tracking and disturbance rejection. The simulation and experimental results are presented, demonstrating the superiority of the HFBC.

**Keywords:** dual star Induction machine • indirect rotor flux oriented control • flatness-based control • hybrid flatness-based control • feedforward controller

## 1. Introduction

Currently, the electrification of embedded systems is subject to a steadily ascending growth, especially in the areas of avionics, marine, and automotive transport. This is within the framework of the policy that aims to solve the environmental problem of global warming which arises in large part because of the harmful gases emitted by industry and current transport systems (Levi, 2008; Levi et al., 2013).

In the aeronautical field, the main focus of research becomes the use of the most recent technology, allowing the reduction of fuel consumption and the mass of equipment, offering a reduction in design and operating costs and maintenance of electrical systems on board the aircraft. This is a desirable objective in the industry.

More electrical aircraft (MEA) means more powerful, more compact, and more reliable on-board systems. The major component in a training chain is the electrical machine and its control. Indeed, the electrification of air transport systems imperatively requires the design of a robust and reliable electric drive (Liu et al., 2018; Nounou et al., 2018). In this context, we see that the electric machines have several advantages compared to internal combustion engines and certain advantages in terms of each of the following: energy reversibility, better efficiency over a wide operating range, ease of integration and absence of gas emissions.

\* Email: nesri\_m@yahoo.fr

The proposed approach is effective for optimising speed and energy efficiency. A control strategy has been developed for improving the trajectory planning based on the theory of flatness. This has demonstrated the possibilities to optimise the dynamic response of the electrical machine and improve the energy delivered by the drive system. Moreover, in high-power and critical applications such as naval propulsion and rail traction, multiphase machines are increasingly used (Levi et al., 2013).

Multi-phase machines have splendid advantages compared to the classical three-phase ones (Liu et al., 2018; Nounou et al., 2018), such as splitting the power across a higher number of phases leading to lower power rating per phase, lower torque ripples due to the improved magneto-motive force distribution in the machine air-gap, fault-tolerant operation according to the high number of degrees of freedom related to the number of independent control variables, and torque density enhancement using harmonic current injection (Barrero and Duran, 2016; Salem and Narimani, 2019).

Generally, multiphase drives control is inspired from that of the three-phase ones. However, these drives are considered complex systems with a higher number of parameters, which leads to uncertainties of their models and, therefore, a lack of control (Baneira et al., 2017; Li et al., 2018). Accordingly, to ensure suitable control with good performances against disturbances and uncertainties, research for more robust control techniques is required (Nesri et al., 2020; Petersen and Tempo, 2014).

In this paper, we have proposed a hybrid control method for the dual star induction machine (DSIM). The proposed control method is a hybridisation between the feedforward control technique based on the concept of flatness feedforward -the flatness-based control (FBC)- and the classical feedback loop control. Direct action is used to drive the system to the desired output by imposing commands calculated from planned reference trajectories. The feedback loop compensates for deviations caused by disturbances and stabilises the system around the reference trajectories. The advantage of this approach is the separation of the objectives of tracking and disturbance rejection, achieved, respectively, by the flatness feedforward control and the feedback loop. It should be noted that the two controls can be designed separately. The flatness theory is used effectively to synthesise an improved electric drive system that is validated experimentally.

The hybrid flatness-based control (HFBC) technique applied to a DSIM as a multi-phase machine is developed, analysed, and compared to the classical indirect rotor-flux oriented control (IRFOC) technique. The FBC is expected to offer more advantages in terms of tracking behaviour, rejection of perturbations, and robustness (Wang et al., 2015, 2019).

In this work, the notion of FBC will be applied in a cascaded structure in the classic IRFOC scheme (as feedforward controller). Indeed, the combination of feedforward and feedback control promises high performance, as the feedforward guarantees reference tracking, while the non-linear feedback element rejects disturbances. The parameter accuracy of the feedforward control significantly affects the control performance of the precision motion system (Ishihara et al., 2020). In the feedback–feedforward control structure, when the feedforward model is equal to the inverse of the controlled plant, the position error can be effectively compensated. To achieve the reference tracking control, a feedback and feedforward control system is established in this paper, as shown in Figure 1. The error between the reference and the feedback signal (measured signal) is processed by the feedback controller to generate the control signal, which is loaded on the motor to generate thrust and the controlled plant moves. The measured position is fed back to the loop to build the closed-loop control, which realises the position tracking control

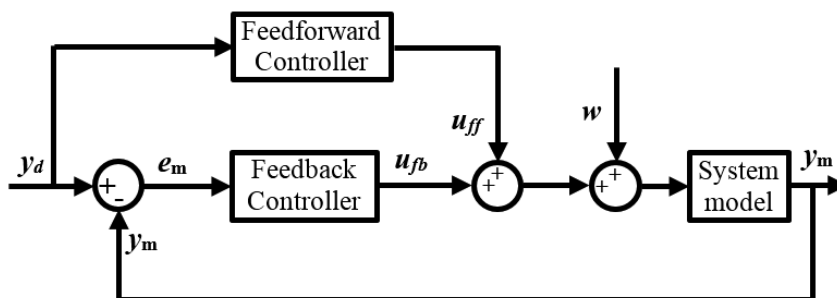


Fig. 1. Feedback–feedforward control configuration.

on the premise of ensuring the stability of the system and has the ability of restraining the disturbance. On this basis, the feedforward control improves the position tracking accuracy by adding an input signal in the forward channel.

Where  $y_d$  denotes the reference or desired output,  $y_m$  denotes the measured output,  $e_m$  denotes the error between the desired and the measured output,  $u_b$  is the feedback control signal,  $u_f$  is the feedforward control signal, and  $w$  is the unknown disturbance.

The main contributions of this paper are listed below:

- Robust control with superior disturbance rejection properties due to the estimation and anticipation of the load torque.
- This robustness can translate into better speed response time; a very short couple establishment period; instant (very quick) disturbance rejection; minimisation of energy supplied for disturbance rejection; and continuity of service in the event of a fault.

The remainder of this paper is organised as follows: The FBC theory and principle are presented in Section 2, the FBC of DSIM is detailed in Section 3, the HFBC of DSIM is detailed in Section 4, and the simulation results are presented and discussed in Section 5. In Section 6, experimental validation is carried out to validate the study on an experimental test bench. Finally, Section 7 concludes the work.

## 2. FBC Theory

The notion of control based on the theory of the differential flatness of systems is a relatively new concept, introduced by Fliess et al. (1992). This concept is based on the choice of the system's flat outputs, and provides a notion of equivalence between a controllable linear system and a non-linear system. Determining the candidate outputs (flat outputs) requires a certain amount of experience with the method and the system to be controlled. However, knowledge of certain flatness criteria can help in the choice of flat outputs (Fliess et al., 1995; Martin and Rouchon, 1996a).

Differential flatness is a property of a non-linear system. Differential flatness is an extension of the term "controllability" for non-linear systems. For linear systems, it is equivalent to controllability, but for non-linear systems, it is a self-standing property. A given dynamical system is either flat or not, depending on whether it fits the following definition of flatness (Martin and Rouchon, 1996a,b).

$$\dot{x} = f(x, u) \quad x \in R^n, u \in R^m \quad (1)$$

where  $x = (x_1, \dots, x_n)$  is the state, and  $u = (u_1, \dots, u_m)$  is the command.

The system (S) is differentially flat if there is a vector 'y' called flat output composed of m outputs  $y = (y_1, \dots, y_m)$  such that:

- the elements of y are differentially independent (the elements of the flat output are not related to each other by a differential equation);
- the state x and the command u are expressed in terms of y and a finite number of its derivatives; and

$$x = h_x(y, \dot{y}, \dots, y^{(\beta)}) \quad (2)$$

$$u = h_u(y, \dot{y}, \dots, y^{(\gamma)}) \quad (3)$$

- the flat output y is expressed as a function of the state x, the command u, and a finite number of derivatives of u.

$$y = h_y(x, u, \dot{u}, \dots, u^{(\alpha)}) \quad (4)$$

where  $\beta$ ,  $\gamma$ , and  $\alpha$  are the orders of derivation of the state x, the command u and the flat output y, respectively.

The first step of the FBC is to define candidate flat outputs, which must satisfy the above conditions (Fliess et al., 1999; Li et al., 2015). After that, the trajectory of the flat outputs is planned with respect to the physical dynamics of the system (Xu et al., 2015). This trajectory is defined in such a way to impose the desired behaviour of the state variables (Li et al., 2015; Xu et al., 2015). The flatness control can be directly used as open loop control in a well-known model. However, this control is commonly extended with an additional control law such as a proportional integral (PI) regulator and sliding controllers in order to enforce the disturbance rejection in the presence of uncertainties (model and operational uncertainties) (Fliess et al., 1995; Li et al., 2015).

### 3. FBC of DSIM

Based on the usual DSIM model (Petersen and Tempo, 2014), the DSIM model is given by the following equation:  
The electrical equations describing the stator and rotor circuits in the  $(\alpha\beta)$  frame are:

$$\begin{cases} V_{s1} = r_{s1}i_{s1} + \frac{d\varphi_{s1}}{dt} \\ V_{s2} = r_{s2}i_{s2} + \frac{d\varphi_{s2}}{dt} \\ 0 = r_r i_r + \frac{d\varphi_r}{dt} \end{cases} \quad (5)$$

$[V_{s1}, V_{s2}, V_r]^T$ : voltage vector ( $V_r = 0$ ).

$[i_{s1}, i_{s2}, i_r]^T$ : current vector.

$[\varphi_{s1}, \varphi_{s2}, \varphi_r]^T$ : flux vector.

$r_s(r_r)$ : matrix of stator resistance (rotor).

Under the assumptions of linearity of the magnetic circuits (valid as long as the stator currents are not too large) and neglecting iron losses, fluxes and currents of the DSIM are expressed as:

$$\begin{cases} \varphi_{s1} = L_{s1}i_{s1} + L_{ms}i_{s2} + M_{sr}i_r \\ \varphi_{s2} = L_{ms}i_{s1} + L_{s2}i_{s2} + M_{sr}i_r \\ \varphi_r = L_r i_r + M_{sr}i_{s1} + M_{sr}i_{s2} \end{cases} \quad (6)$$

Where  $L_s$  and  $L_r$  are the stator and the rotor inductance matrix, respectively,  $L_{ms}$  the mutual inductance matrix between the two stars of the stator, and  $M_{sr}$  the mutual inductance matrix between the stator and the rotor.

The  $dq$  frame is linked to the  $\alpha\beta$  one according to  $x_{\alpha\beta} = x_{dq}e^{j\delta}$  (Chitra and Prabhakar, 2006; Marino et al., 1993). As a consequence of the Lorenz force law, the electromagnetic torque is given by (Chiasson, 1996):

$$T_e = p \frac{M_{sr}}{L_r} \text{Im}[\bar{I}_s \cdot \vec{\varphi}_r^*] \quad (7)$$

$$T_e = p \frac{1}{R_r} \rho^2 \dot{\alpha} \quad (8)$$

where  $\alpha$  is the rotor-flux phase in the rotor frame ( $\varphi_r = \rho e^{j\alpha}$ );  $\rho$  and  $\delta$  are, respectively, the rotor-flux modulus and argument in the fixed frame, ( $\alpha = \delta - p\theta$ ); where  $p$  is the number of the pole pairs; and we denote by  $j$  the pure imaginary number satisfying  $j^2 = -1$ .

The mechanical equation is written as follows:

$$J \frac{d\Omega}{dt} = T_e - T_L - k_f \Omega \quad (9)$$

where  $J$  is the rotor moment of inertia,  $k_f$  is the coefficient of friction, and  $T_L$  is the external load torque.

$$J \frac{d\Omega}{dt} = p \frac{1}{R_r} \rho^2 \dot{\alpha} - T_L - k_f \Omega \quad (10)$$

$$\dot{\alpha} = \frac{R_r}{p \cdot \rho^2} \left( J \frac{d\Omega}{dt} + T_L + k_f \Omega \right) \quad (11)$$

in a reference frame called ( $d$ - $q$ ), where the rotor flux is oriented along the  $d$  axis and after substitutions and mathematical manipulations, we obtain the *feedforward* action commands:

- Direct action of current (*current feedforward*)

$$\begin{cases} i_{sd1} = \frac{1}{2M_{sr}} [\rho + T_r \dot{\rho}] \\ i_{sd2} = \frac{1}{2M_{sr}} [\rho + T_r \dot{\rho}] \\ i_{sq1} = \frac{T_r}{2M_{sr}} \rho \dot{\alpha} \\ i_{sq2} = \frac{T_r}{2M_{sr}} \rho \dot{\alpha} \end{cases} \quad (12)$$

such that

$$\sigma_s = \left( 1 - \frac{M_{sr}^2}{L_s L_r} \right), \quad \sigma_m = \left( 1 - \frac{M_{sr}^2}{L_{ms} L_r} \right)$$

- Direct action of voltage (*voltage feedforward*)

$$\begin{cases} V_{sd1} = R_s I_{sd1} + L_s \sigma_s \dot{I}_{sq1} + L_s \sigma_s \frac{dI_{sd1}}{dt} + L_{ms} \sigma_m \dot{I}_{sq2} + L_{ms} \sigma_m \frac{dI_{sd2}}{dt} + \frac{M_{rs}}{L_r} \dot{\rho} \\ V_{sq1} = R_s I_{sq1} - L_s \sigma_s \dot{I}_{sd1} + L_s \sigma_s \frac{dI_{sq1}}{dt} - L_{ms} \sigma_m \dot{I}_{sd2} + L_{ms} \sigma_m \frac{dI_{sq2}}{dt} + \frac{M_{rs}}{L_r} \rho \dot{\delta} \\ V_{sd2} = R_s I_{sd2} + L_s \sigma_s \dot{I}_{sq2} + L_s \sigma_s \frac{dI_{sd2}}{dt} + L_{ms} \sigma_m \dot{I}_{sq1} + L_{ms} \sigma_m \frac{dI_{sd1}}{dt} + \frac{M_{rs}}{L_r} \dot{\rho} \\ V_{sq2} = R_s I_{sq2} - L_s \sigma_s \dot{I}_{sd2} + L_s \sigma_s \frac{dI_{sq2}}{dt} - L_{ms} \sigma_m \dot{I}_{sd1} + L_{ms} \sigma_m \frac{dI_{sq1}}{dt} + \frac{M_{rs}}{L_r} \rho \dot{\delta} \end{cases} \quad (13)$$

The DSIM is a flat system; all state variables are expressed as a function of the flat outputs and their derivatives. In other words, the trajectory of the vector planned by the flat outputs determines the trajectory of the whole state of the system. Therefore, it determines the behaviour of the system. The dynamics of the stator currents are much faster than that of the speed and the flux. An internal current regulation loop can be designed from Eqs (5) and (6), assuming that the speed and the rotor flux are constant; the flat outputs, therefore, considered for stator current regulations are  $y_1 := (i_{s1}, i_{s2})$ ; if we impose a trajectory for the currents, we can deduce the reference voltages to control the machine through the Eq (13). For the external speed and flux regulation loop, the stator currents are considered the new control inputs. This system is also flat with  $y_2 := (\rho, \Omega)$ ; if we impose a trajectory for speed and rotor flux, we can deduce the reference currents through Eq (12). For the flat output, the trajectory is often designed with respect to the control objective. This corresponds to a known function of time  $t \rightarrow y$  on a given time interval  $[t; t_f]$  (Jin and Zhao, 2019). The objective set through this command is to monitor the rotor speed profile while maintaining

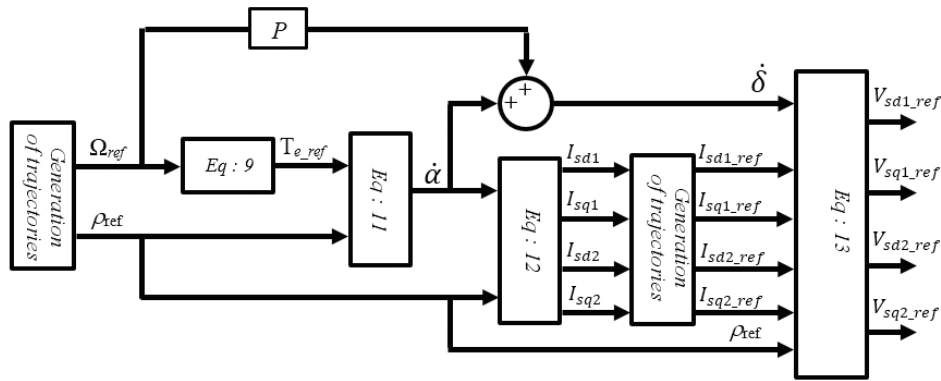


**Fig. 2.** FBC of DSIM scheme.

constant flux in the machine and rejection of closed-loop disturbances. As already mentioned, the feedforward is only effective if the references are smooth enough. Thus, the reference trajectory generation is very important for the FBC. The presence of derivations requires the application of filters to the reference of flat outputs  $y_1$  and  $y_2$ . In this paper, besides a first-order filter, a rate limiter with different settings is investigated by simulations. Additionally, it would be desirable to include the limitations in the control inputs directly into the reference trajectory generation (Martin et al., 2006; Ortega et al., 2001). Then, the DSIM model achieves all the conditions of a flat system which were mentioned previously. The elements of  $y$  are differentially independent. Figure 2 shows the DSIM FBC scheme.

## 4. HFBC of DSIM

The flatness property (Chitra and Prabhakar, 2006; Marino et al., 1993) can be used effectively to design control algorithms. In general, the HFBC of the DSIM scheme consists of two parts (feedback and feedforward actions) (Chiasson, 1996). The flatness control allows the control inputs to be formulated as functions of the flat outputs only; this can be used to develop the direct action inputs. Under ideal conditions, the feedforward can follow the reference, if it is sufficiently smooth. Otherwise, due to derivatives in the references and limitations in the control, input tracking errors would appear. Even if the references are sufficiently smooth, deviations from perfect tracking appear due to operating disturbances, model uncertainties, and other unknown disturbances; therefore, feedback action is introduced (Jin and Zhao, 2019; Salem and Narimani, 2019).

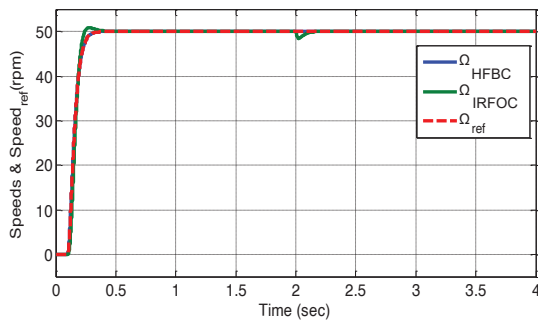
The hybrid control technique based on the flatness theory is a combination of feedforward control based on the concept of flatness and conventional IRFOC vector control (the feedback loop) (Fliess et al., 1995; Martin and Rouchon, 1996a,b). Direct action drives the system to the desired output by imposing commands calculated from planned reference trajectories. The feedback loop compensates for deviations caused by disturbances and stabilises the system around the reference trajectories. The advantage of this approach is the separation of the objectives of tracking and disturbance rejection, achieved respectively by the flatness feedforward control and the feedback loop. Note that the two controls can be designed separately. Figure 3 illustrates the principle of HFBC.

The HFBC scheme is designed by adding to the conventional IRFOC scheme a current feed-forward controller and a voltage feedforward controller (Fan and Zhang, 2011; Singh et al., 2020). The two feedforward controllers are designed based on the method of flatness input. The outputs of the feedback regulators are always zero except in the case of the presence of a disturbance.

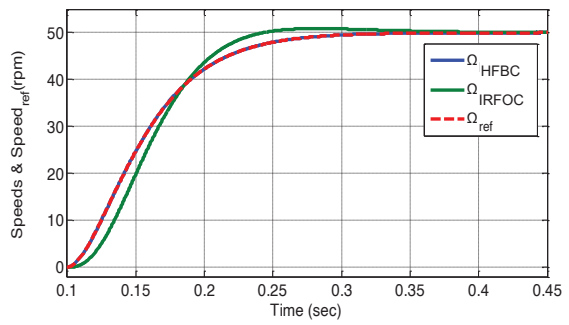
## 5. Simulation Results

A comparison of the two control techniques performances is presented in this section. The parameters of the simulated machine are the same as those of the experimental one, which are shown in the Appendix.

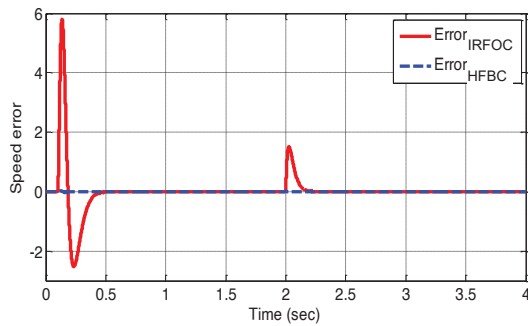




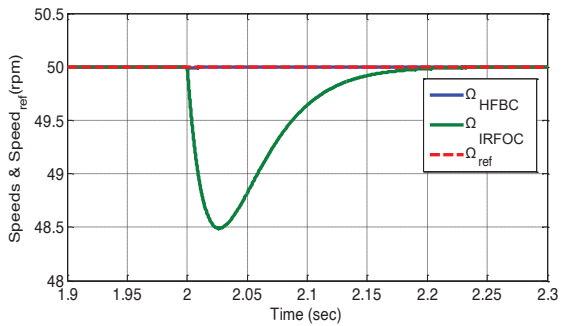
(a) Speed curves



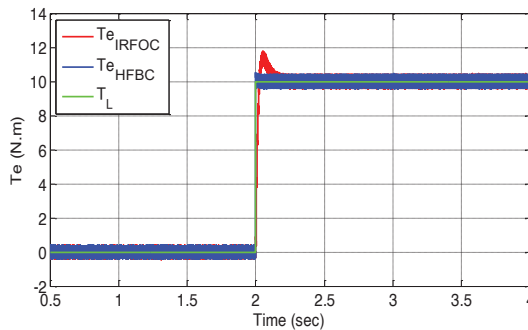
(a') Speed curves (Zoom 1)



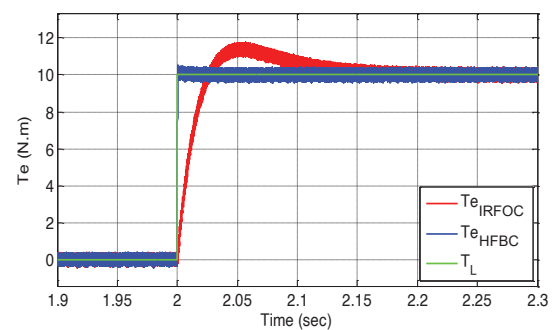
(b) Speed error curves



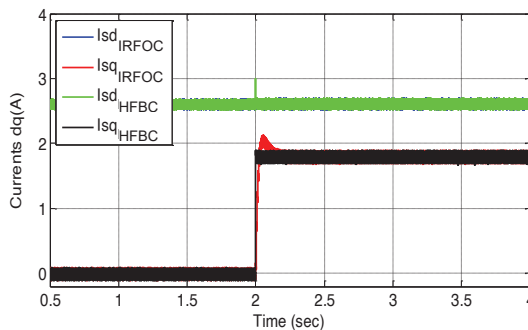
(a'') Speed curves (Zoom 2)



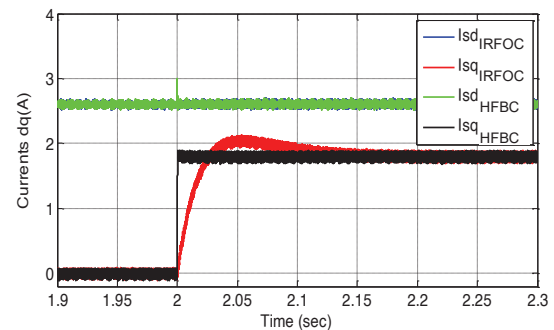
(c) Electromagnetic torque curves



(c') Electromagnetic torque curves (Zoom)



(d) First star currents (d-q) components curves



(d') First star currents (d-q) components curves (Zoom)

**Fig. 4.** DSIM IRFOC and HFBC simulation results.

The experimental results of Figures 5a and 5a' confirm those of the simulation and show that the HFBC technique exhibits better dynamic performances. From Figure 5a'', it can be seen that the HFBC has favourable performances in terms of stabilisation time compared with IRFOC such that the speed establishing time is equal to 5.5 s for IRFOC

Parameters of comparison (s)	IRFOC	HFBC
Speed establishing time (s)	0.35	0.024
$t_{r_{(95\%)}}$ (s)	0.12	0.14
Speed drop relative to a load torque (%)	3	0.04
Speed compensation time relative to a load torque (s)	0.27	0.03
Speed overrun (%)	2	0
Torque establishing time	0.3 s	0.3 ms
Torque overrun (%)	15	Negligible

**Table 1.** Simulation performances comparison of IRFOC and HFBC.

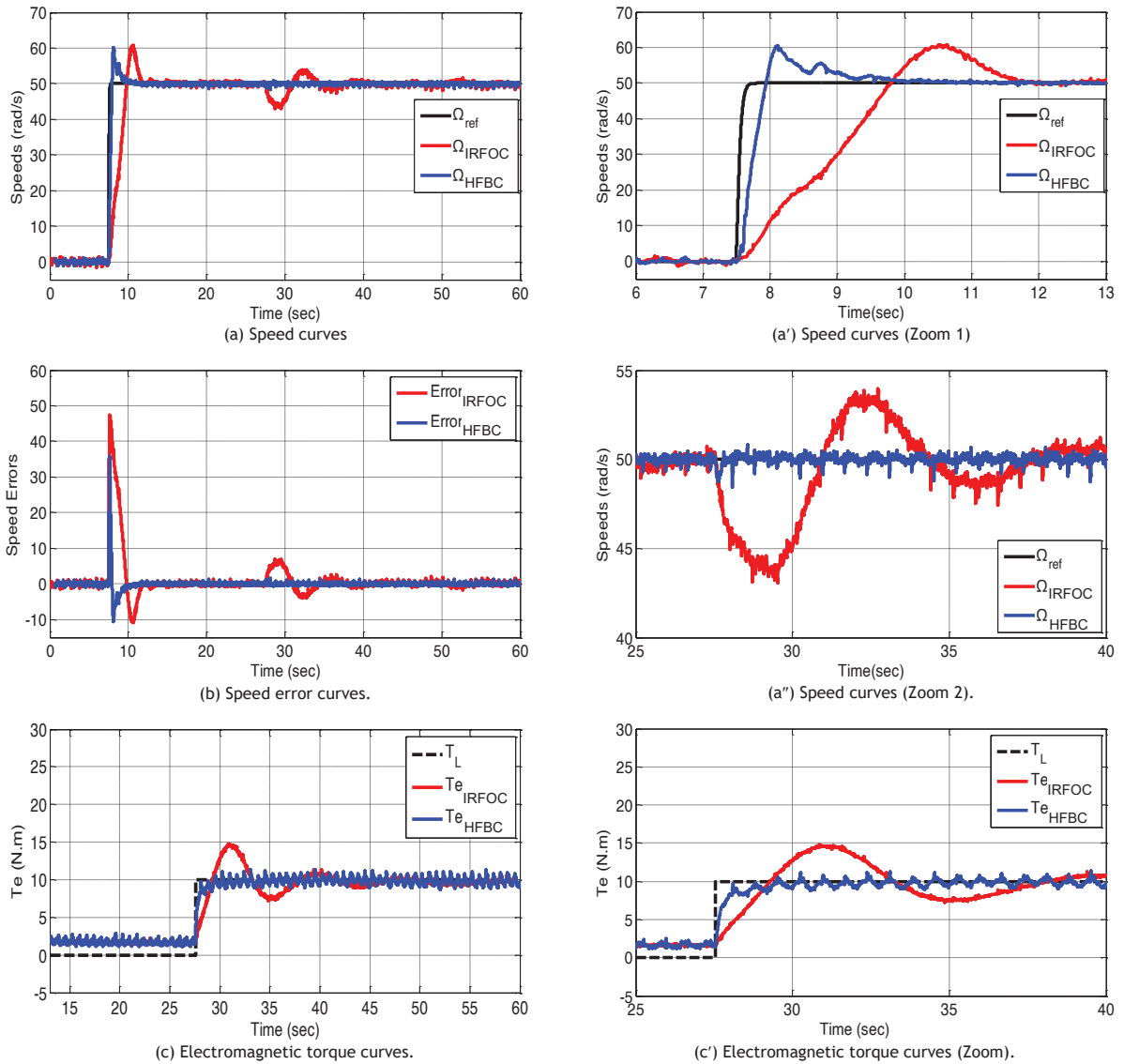


**Fig. 5.** Continued

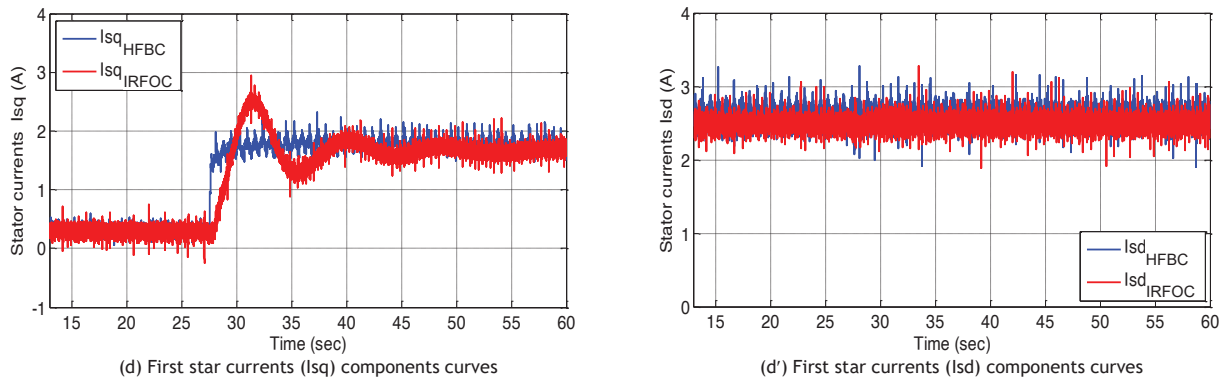


**Fig. 5.** DSIM IRFOC and HFBC experimental results.

Parameters of comparison	IRFOC	HFBC
Speed establishing time (s)	5.5	2.5
$t_r$ (95%) (s)	2.2	0.43
Speed drop relative to a load torque (%)	12	2.2
Speed compensation time relative to a load torque (s)	12.5	0.15
Speed overrun (%)	21.5	21
Torque establishing time (s)	17.5	5
Torque overrun (%)	45.7%	Negligible

**Table 2.** Experimental performances comparison of IRFOC and HFBC.

and equal to 2.5 s for the HFBC. It is also noted that the HFBC shows better performances against the rejection of disturbances compared to the IRFOC.

The application of the load torque  $T_L = 10$  Nm causes a speed drop equal to 12% for the IRFOC and 2.2% for the HFBC. This speed drop is compensated after 12.5 s for the IRFOC and after only about 0.15 s in the case of the HFBC. Accordingly, the application of a load torque has no significant effects on the performances of the drive speed control with the HFBC. It is also noted that the speed trajectory following errors are approximately zero in the steady state for the HFBC. However, the maximum speed error is approximately about 47 rad/s for IRFOC and 34 rad/s for HFBC, as shown in Figure 5b. The HFBC presents a good dynamic tracking of the current components ( $dq$ ) as illustrated in Figures 5d and 5d', respectively. A comparison of the main performances evaluation parameters of each control method is summarised in Table 2.

## 7. Conclusion

The FBC strategy combined with an IRFOC method applied to a power drive system is presented in this paper. The presented results show that a hybrid control method based on the flatness theory can be a very attractive solution for devices using DSIM such as electric/hybrid vehicles and electrical aircraft. The simulation and experimental results show that the HFBC offers higher performances in steady and transient states, even in the presence of perturbations and parameter variations, compared to the classical vector control technique. Moreover, an enhancement of the drive system control performances is demonstrated by the improvement of the technique of the separation of the objectives of tracking and disturbance rejection (achieved, respectively, by the flatness *feedforward* control and the feedback loop). In addition, the HFBC principle and experimental implementation are simple and can be generalized and applied to the control of other power systems, and the control methodology proposed here is also such that it would be simple to extend it to other electric motors. Future work will address the fault-tolerant control and the implementation of the artificial intelligence controllers.

## References

- Baneira, F., Doval-Gandoy, J., Yepes, A. G., López, Ó. and Pérez-Estévez, D. (2017). Control Strategy for Multiphase Drives with Minimum Losses in the Full Torque Operation Range under Single Open-Phase Fault. *IEEE Transactions on Power Electronics*, 32(8), pp. 6275–6285. doi: 10.1109/TPEL.2016.2620426.
- Barrero, F. and Duran, M. J. (2016). Recent Advances in the Design, Modeling, and Control of Multiphase Machines – Part I. *IEEE Transactions on Industrial Electronics*, 63(1), pp. 449–458. doi: 10.1109/TIE.2015.2447733.
- Chiasson, J. (1996). Nonlinear Controllers for an Induction Motor. *Control Engineering Practice*, 4(7), pp. 977–990. doi: 10.1016/0967-0661(96)00097-4.
- Chitra, V. and Prabhakar, R. (2006). Induction motor speed control using fuzzy logic controller. *World Acad. Sci. Eng. Technol.* 2006, 23, 17–22.
- Dannehl, J. and Fuchs, F.W. (2006). Flatness-based control of an induction machine fed via voltage source inverter-concept, control design and performance analysis. In *Proceedings of the IECON 2006-32nd Annual Conference on IEEE Industrial Electronics*, Paris, France, 6–10 November 2006; pp. 5125–5130.
- Fan, L. and Zhang, L. (2011). An Improved Vector Control of an Induction Motor Based on Flatness. *Procedia Engineering*, 15, pp. 624–628. doi: 10.1016/j.proeng.2011.08.116.
- Fliess, M., Levine, J., Martin, P. and Rouchon, P. (1995). Flatness and Defect of Non-Linear Systems: Introductory Theory and Examples. *International Journal of Control*, 61(6), pp. 1327–1361. doi: 10.1080/00207179508921959.
- Fliess, M., Lévine, J., Martin, P. and Rouchon, P. (1999). A Lie-Bäcklund Approach to Equivalence and Flatness of Nonlinear Systems. *IEEE Transactions on Automatic Control*, 44(5), pp. 922–937. doi: 10.1109/9.763209.
- Ishihara, S., Tahara, K. and Hironaka, K. (2020). Feedforward Control Design for Shaking Table by Data Driven Control Considering Control Input Limitation. *IFAC-PapersOnLine*, 53(2), pp. 9011–9016. doi: 10.1016/j.ifacol.2020.12.2019.
- Jin, H. Y. and Zhao, X. M. (2019). Extended Kalman Filter-Based Disturbance Feed-Forward Compensation Considering Varying Mass in High-Speed Permanent Magnet Linear Synchronous Motor. *Electrical Engineering*, 101(2), pp. 537–544. doi: 10.1007/s00202-019-00802-z.
- Levi, E. (2008). Multiphase Electric Machines for Variable-Speed Applications. *IEEE Transactions on Industrial Electronics*, vol. 55, no. 5, pp. 1893–1909, May 2008.
- Levi, E., Bodo, N., Dordevic, O., Jones, M. (2013). Recent advances in power electronic converter control for multiphase drive systems. In *Proceedings of the 2013 IEEE Workshop on Electrical Machines Design, Control and Diagnosis (WEMDCD)*, Paris, France, 11–12 March 2013; pp. 158–167.
- Li, S., Fang, Z., Fukui, Y., Futatsukawa, K., Mizobata, S., Qiu, F., Sato, Y. and Shinozaki, S. (2018). Adaptive feedforward control design Based on Simulink for J-Parc Linac LLRF system. In: *9th International Particle Accelerator Conference*, Vancouver, BC, Canada, pp. 2187–2189.
- Li, T., Xia, Y. and Ma, D. (2015). Flatness-Based Target Tracking for a Quadrotor Unmanned Aerial Vehicle. *IFAC-PapersOnLine*, 48(28), pp. 874–879. doi: 10.1016/j.ifacol.2015.12.240.
- Liu, Z., Li, Y. and Zheng, Z. (2018). A Review of Drive Techniques for Multiphase Machines. *CES Transactions on Electrical Machines and Systems*, 2(2), pp. 243–251. doi: 10.30941/cestems.2018.00030.
- Marino, R., Peresada, S. and Valigi, P. (1993). Adaptive Input-Output Linearizing Control of Induction Motors. *IEEE Transactions Automatic Control*, 38(2), pp. 208–221. doi: 10.1109/9.250510.
- Martin, P., Rouchon, P. and Murray, R. M. (2006). Flat systems, equivalence and trajectory generation. 3rd cycle. Castro Urdiales (Espagne), France. 2006, pp. 81. cel-00392180
- Martin, P. and Rouchon, P. (1996a). Flatness and Sampling Control of Induction Motors. *IFAC Proceedings Volumes*, 29(1), pp. 2786–2791. doi: 10.1016/s1474-6670(17)58098-2.
- Martin, P. and Rouchon, P. (1996b). Two Remarks on Induction Motors. In: *CESA'96 IMACS Multiconference*. 1996. p. 76-9.
- Nesri, M., Nounou, K., Marouani, K., Houari, A. and Benkhoris, M. F. (2020). Efficiency Improvement of a Vector-Controlled Dual Star Induction Machine Drive System. *Electrical Engineering*, 102(2), pp. 939–952. doi: 10.1007/s00202-020-00924-9.
- Nounou, K., Benbouzid, M., Marouani, K., Charpentier, J. F. and Kheloui, A. (2018). Performance Comparison of Open-Circuit Fault-Tolerant Control Strategies for Multiphase Permanent Magnet Machines for Naval Applications. *Electrical*

- Engineering, 100(3), pp. 1827–1836. doi: 10.1007/s00202-017-0661-9.
- Ortega, R., Louis, J. and Delaleau, E. (2001). Modeling and Control of Induction Motors. *International Journal of Applied Mathematics and Computer Science*, 11(1), pp. 105–129. doi: NODOI.
- Petersen, I. R. and Tempo, R. (2014). Robust Control of Uncertain Systems: Classical Results and Recent Developments. *Automatica*, 50(5), pp. 1315–1335. doi: 10.1016/j.automatica.2014.02.042.
- Salem, A. and Narimani, M. (2019). A Review on Multiphase Drives for Automotive Traction Applications. *IEEE Trans. Transp. Electrification*, 5(4), pp. 1329–1348. doi: 10.1109/TTE.2019.2956355.
- Singh, K. V., Bansal, H. O. and Singh, D. (2020). Feed-Forward Modeling and Real-Time Implementation of an Intelligent Fuzzy Logic-Based Energy Management Strategy in a Series–Parallel Hybrid Electric Vehicle to Improve Fuel Economy. *Electrical Engineering*, 102(2), pp. 967–987. doi: 10.1007/s00202-019-00914-6.
- Wang, K., Zhu, Z. Q., Ren, Y. and Ombach, G. (2015). Torque Improvement of Dual Three-Phase Permanent-Magnet Machine with Third-Harmonic Current Injection. *IEEE Transactions on Industrial Electronics*, 62(11), pp. 6833–6844. doi: 10.1109/TIE.2015.2442519.
- Wang, X., Wang, Z., Xu, Z., Cheng, M., Wang, W. and Hu, Y. (2019). Comprehensive Diagnosis and Tolerance Strategies for Electrical Faults and Sensor Faults in Dual Three-Phase PMSM Drives. *IEEE Transactions on Power Electronics*, 34(7), pp. 6669–6684. doi: 10.1109/TPEL.2018.2876400.
- Xu, Y., Li, F., Jin, Z. and Huang, C. (2015). Flatness-Based Adaptive Control (FBAC) for STATCOM. *Electric Power Systems Research*, 122, pp. 76–85. doi: 10.1016/j.epsr.2014.12.023.

## Appendix

Quantity	Symbol and magnitude
Rated Power	$P_n = 5.5 \text{ kW}$
Rated voltage	$V_n = 110 \text{ V}$
Rated current	$I_n = 6 \text{ A}$
Rated speed	$N_n = 950 \text{ rpm}$
Number of poles	$2 \cdot p = 6$
Rated Frequency	$f = 50 \text{ Hz}$
Stator resistance	$R_s = 2.03 \ \Omega$
Rotor resistance	$R_r = 3 \ \Omega$
Stator inductance	$L_s = 0.215 \text{ H}$
Rotor inductance	$L_r = 0.215 \text{ H}$
Mutual inductance	$M = 0.2 \text{ H}$
Moment of inertia	$J = 0.06 \text{ kg.m}^2$
Coefficient of viscous friction	$k_f = 0.006 \text{ N.m.s/rad}$

**Table A1.** Dual star induction machine parameters.

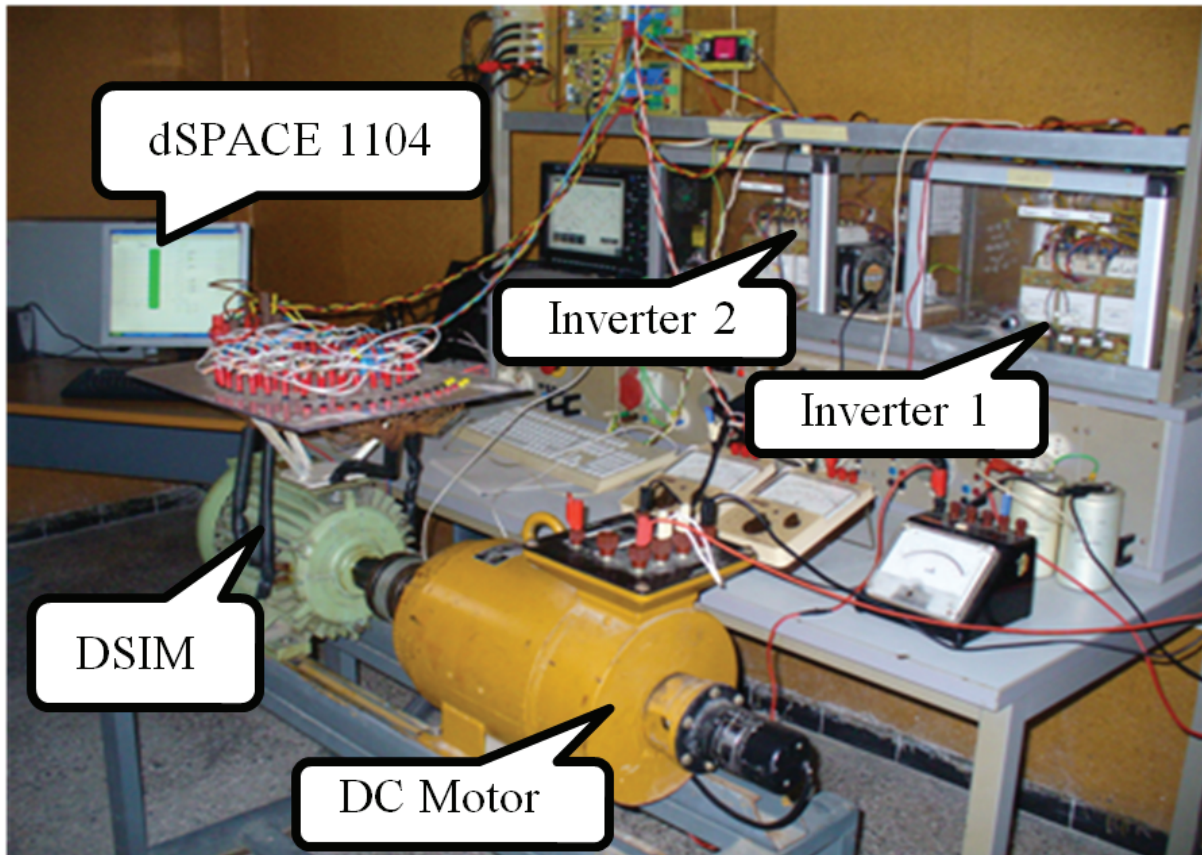


**Fig. A1.** Photography of the experimental test bench.